Isolation and Characterization of Limonoids from *Kigelia africana*

Bushra Jabeen[a], Naheed Riaz[a], Muhammad Saleem[a], Muhammad Akram Naveed[a], Maqsood Ahmed[a], Muhammad Nawaz Tahir[b], Gennaro Pescitelli[c], Muhammad Ashraf[d], Syeda Abida Ejaz[e], Irshad Ahmed[e], and Abdul Jabbar[a]

[a] Department of Chemistry, Baghdad-ul-Jadeed Campus, The Islamia University of Bahawalpur, Bahawalpur 63100, Pakistan
[b] Department of Physics, University of Sargodha, Sargodha, Pakistan
[c] Department of Chemistry, University of Pisa, via Risorgimento 35, I-56126, Pisa, Italy
[d] Department of Biochemistry and Biotechnology, Baghdad-ul-Jadeed Campus, The Islamia University of Bahawalpur, Bahawalpur 63100, Pakistan
[e] Department of Pharmacy, Khawaja Fareed Campus, The Islamia University of Bahawalpur, Bahawalpur 63100, Pakistan

Reprint requests to N. Riaz. E-mail: nrch322@yahoo.com or nrch322@hotmail.com

Z. Naturforsch. **2013**, *68b*, 1041 – 1048 / DOI: 10.5560/ZNB.2013-3096
Received April 19, 2013

Two new limonoids, 1-*O*-deacetyl-2α-methoxykhayanolide (**1**) and kigelianolide (**2**), together with deacetylkhayanolide E (**3**), 1-*O*-deacetyl-2α-hydroxykhayanolide E (**4**) and khayanolide B (**5**) were isolated from the ethyl acetate-soluble fraction of the methanolic extract of *Kigelia africana*. The structures of these limonoids (**1**–**5**) were elucidated by the combination of 1D (^{1}H and ^{13}C NMR) and 2D (HMQC, HMBC and COSY) NMR spectroscopy and mass spectrometry (EIMS, HREIMS), and in comparison with literature data of related compounds. The structure of compound **1** was further confirmed by X-ray crystallography, and the absolute stereochemistry of compounds **1** and **2** was determined by electronic circular dichroism (ECD) spectroscopy. Limonoids **1**–**5** showed weak inhibitory activities against the enzymes acetylcholinesterase (AChE), butyrycholinesterase (BChE) and lipoxygenase (LOX) in a concentration-dependent manner with IC_{50} values in the ranges 137.5 – 225.2 μM for AChE, 185.4 – 241.5 μM for BChE and 281.2 – 189.6 μM for LOX.

Key words: *Kigelia africana*, Methanolic Extract, Limonoids, Solid-state ECD/TDDFT Method, Enzyme Inhibition

Introduction

Kigelia africana belongs to the family Bignoniaceae, which is an African plant, commonly found in South, Central and West Africa [1]. Its crushed dried fruits are used in folk medicine as emollient, anti-eczema, anti-psoriasis and skin-firming agent and as dressing for ulcers and wounds. The root bark is used for the treatment of venereal disesases, haemorrhoids and rheumatism [2]. The naphthoquinones [3] in the roots and stem bark of *K. africana* possess anti-trypanosomal [4] and anti-microbial activities [5] and are cytotoxic against melanoma and renal carcinoma cells [6]. The aqueous extract of its leaves and fruits was found to have anti-diarrhoeal, anti-leprotic, anti-malarial, and anti-implantation activities [7]. The whole plant is accounted for its analgesic, anti-inflammatory, anti-molluscidal and anti-oxidative properties [8, 9]. The root bark is recommended for the treatment of various kinds of cancer [10], gynecological problems and to cure rheumatism, dysentery, haemorrhages, diabetes, pneumonia, toothache, and veneral diseases [11]. A literature survey revealed that iridoids, naphthoquinones, monoterpenoidnaphthoquinones, isocoumarins, lignans, sterols, and flavonoids have been identified from the genus *Kigelia* [12]. Herein we report the isolation and structural elucidation of two new limonoids, namely 1-*O*-deacetyl-2α-methoxykhayanolide (**1**) and kigelianolide (**2**), together with deacetylkhayanolide E (**3**) [13], 1-*O*-deacetyl-2α-hydroxykhayanolide E (**4**) [14], and khayanolide B (**5**) [15] from the

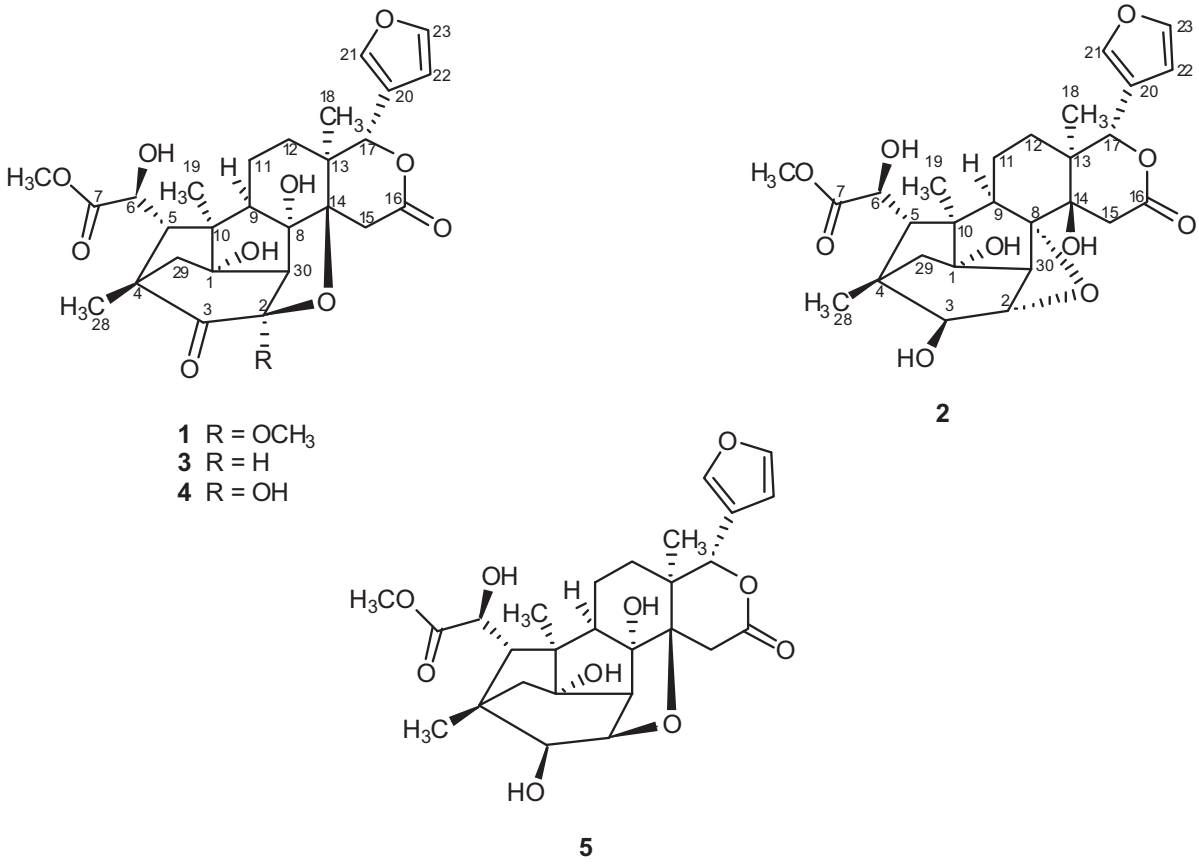

Fig. 1. Structures of limonoids **1**–**5** isolated from *Kigelia africana*.

ethyl acetate-soluble fraction of *Kigelia africana* (Fig. 1).

Results and Discussion

1-*O*-Deacetyl-2α-methoxykhayanolide E (**1**) was obtained as a crystalline solid. The IR spectrum showed the presence of O–H (3435 cm^{-1}), C=O (1736, 1718 cm^{-1}) and C=C (1615 cm^{-1}) groups. Its molecular formula $C_{28}H_{34}O_{11}$ was deduced by HREIMS ($m/z = 546.2110$) with 12 double bond equivalents (DBE). The ^{1}H NMR spectrum of **1** (Table 1) showed three tertiary methyls at $\delta = 1.32$, 1.07 and 1.01, two oxygenated methyls at $\delta = 3.71$ and 3.48, (3H each, s), oxygenated methines at $\delta = 5.51$ (1H, s) and 4.22 (1H, d, $J = 8.4$ Hz), various signals between $\delta = 0.94 - 2.89$ for cyclic methylenes and methines and a furan moiety at $\delta = 7.54$, 7.49, 6.46 (1H each, s). The ^{13}C NMR spectrum of **1** (Table 1) supported the above data as it displayed a total of 28 carbon resonances for five methyl ($\delta = 53.1$, 52.7, 18.7, 15.7, 15.6), four methylene ($\delta = 43.8$, 37.5, 28.8, 17.2), eight methine ($\delta = 144.2$, 142.7, 111.1, 82.5, 73.7, 71.5, 56.8, 44.1), and eleven quaternary carbon atoms ($\delta = 204.7$, 175.5, 173.9, 122.1, 101.9, 88.3, 86.4, 84.9, 61.0, 50.2, 38.7). The above spectroscopic data are very similar to those of 1-*O*-deacetyl-2α-hyroxykhayanolide E [14] indicating that both compounds have the same carbon framework. The only difference lies in the increased molecular weight of **1** by 14 units which was attributed to the presence of a methoxy group in **1** instead of the hydroxy group in the reference compound 1-*O*-deacetyl-2α-hydroxykhayanolide E (**4**) with the molecular formula $C_{27}H_{32}O_{11}$. The position of the methoxy group was confirmed at C-2 through an HMBC spectrum, in which the methoxy protons ($\delta = 3.48$) showed a ^3J correlation with C-2 ($\delta = 101.9$). The remaining sub-

Table 1. ^{1}H and ^{13}C NMR data, HMBC, and COSY correlations of **1** (CD_3OD).

Position	δ_H (mult., J in Hz)	δ_C	HMBC (H→C)	COSY (H→H)
1	–	84.9	–	–
2	–	101.9	–	–
3	–	204.7	–	–
4	–	50.2	–	–
5	2.89 (d, 8.4)	44.1	1,4,6,7,10,19,28,29	H-5/H-6
6	4.22 (d, 8.4)	71.5	4,5,7,10	H-6/H-5
7	–	175.5	–	–
8	–	88.3	–	–
9	2.28 (d, 9.0)	56.8	1,5,8,11,12,14,19,30	H-9/H-11
–	–	61.0	–	–
11	1.97 (d, 13.8) 1.81 (dd, 14.1, 5.4)	17.2	8,9,10,12,13	H-11/H-9,12
12	1.73 (dt, 13.8, 3.0) 0.94 (d,12.0)	28.8	9,11,13,14,18	H-12/H-11
13	–	38.7	–	–
14	–	86.4	–	–
15	3.19 (s)	37.5	8,13,14,16	–
16	–	173.9	–	–
17	5.51 (s)	82.5	12,13,14,18,20,21,22	–
18	1.07 (s)	15.7	12,13,14,17	–
19	1.32 (s)	18.7	1,5,9,10	–
20	–	122.1	–	–
21	7.54 (s)	142.7	17,20,22,23	–
22	6.46 (s)	111.1	17,20,21,23	–
23	7.49 (s)	144.2	20,21,22	–
28	1.01 (s)	15.6	3,4,5,29	–
29	2.10 (d, 12.6) 1.85 (d, 12.6)	43.8	1,3,4,5,10,30	H-29a/H-29b
30	2.86 (s)	73.7	1,2,3,8,9,14,29	–
2-OMe	3.48 (s)	53.1	2	–
7-OMe	3.71 (s)	52.7	7	–

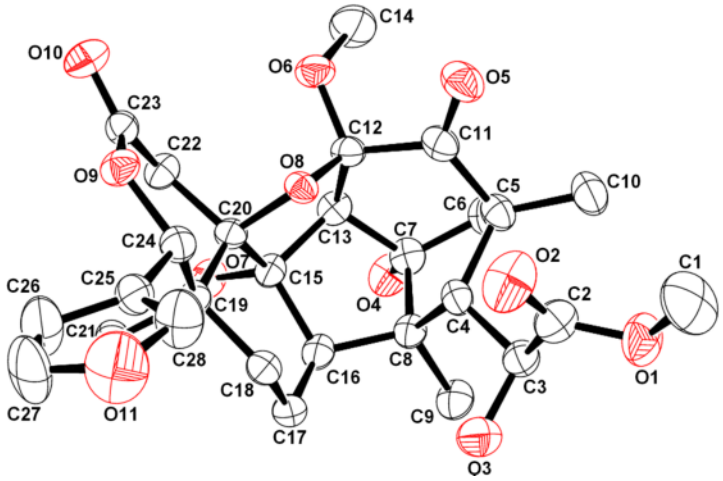

Fig. 2 (color online). ORTEP3 diagram of the molecular structure of **1** in the crystal and atom numbering scheme adopted. The interstitial water molecule was omitted for clarity.

stitution pattern was confirmed by the combination of HMQC, HMBC and COSY correlations. The structure was also confirmed by X-ray crystallography (Fig. 2).

The absolute configuration of **1** could be established by means of the so-called solid-state ECD/TDDFT method [16]. It consists of comparing the electronic circular dichroism (ECD) spectrum measured on a microcrystalline sample with that calculated by means of time-dependent density functional theory (TDDFT) [17] using the X-ray coordinates as input

structure. This approach renders a full conformational analysis unnecessary [18] and is especially useful in assigning the absolute configuration of flexible natural products. In the case of compound **1**, the rotation of the furan chromophore around the C17–C20 bond, which is expected to affect the ECD spectrum, is frozen in the crystals. In Fig. 3 (left) the experimental absorption and ECD spectra of (+)-**1** measured in acetonitrile solution and in the solid state, as KCl pellet, are displayed. The solid-state spectrum shows a long-wavelength cut-off because of the strong furan absorption. However, the positive ECD band around 305 nm is consistently found both in solution and in the solid state. In Fig. 3 (right) the calculated spectra are shown, employing the TDDFT method at the CAM-B3LYP/TZVP level (other functional/basis set combinations gave consistent results). The X-ray geometry was used as input structure with an initially arbitrary (1*S*,2*R*,4*R*,5*R*,6*S*,8*S*,9*R*,10*S*,13*S*,14*R*,17*S*,30*S*) configuration, after optimization of hydrogen atoms only (see Experimental Section). The calculated ECD spectrum nicely reproduces the experimental one; in particular, the band calculated at 302 nm has a positive sign for the above configuration. This band is associated with an n-π^* transition mainly localized on the C3 carbonyl group, which is quite distant from the furan and depends only on the rigid ring system. Based on the above discussion, the compound was assigned the structure (1*S*,2*R*,4*R*,5*R*,6*S*,8*S*,9*R*,10*S*,13*S*,14*R*,17*S*,30*S*)-**1** and named 1-*O*-deacetyl-2α-methoxykhayanolide E. The assigned absolute configuration corresponds to

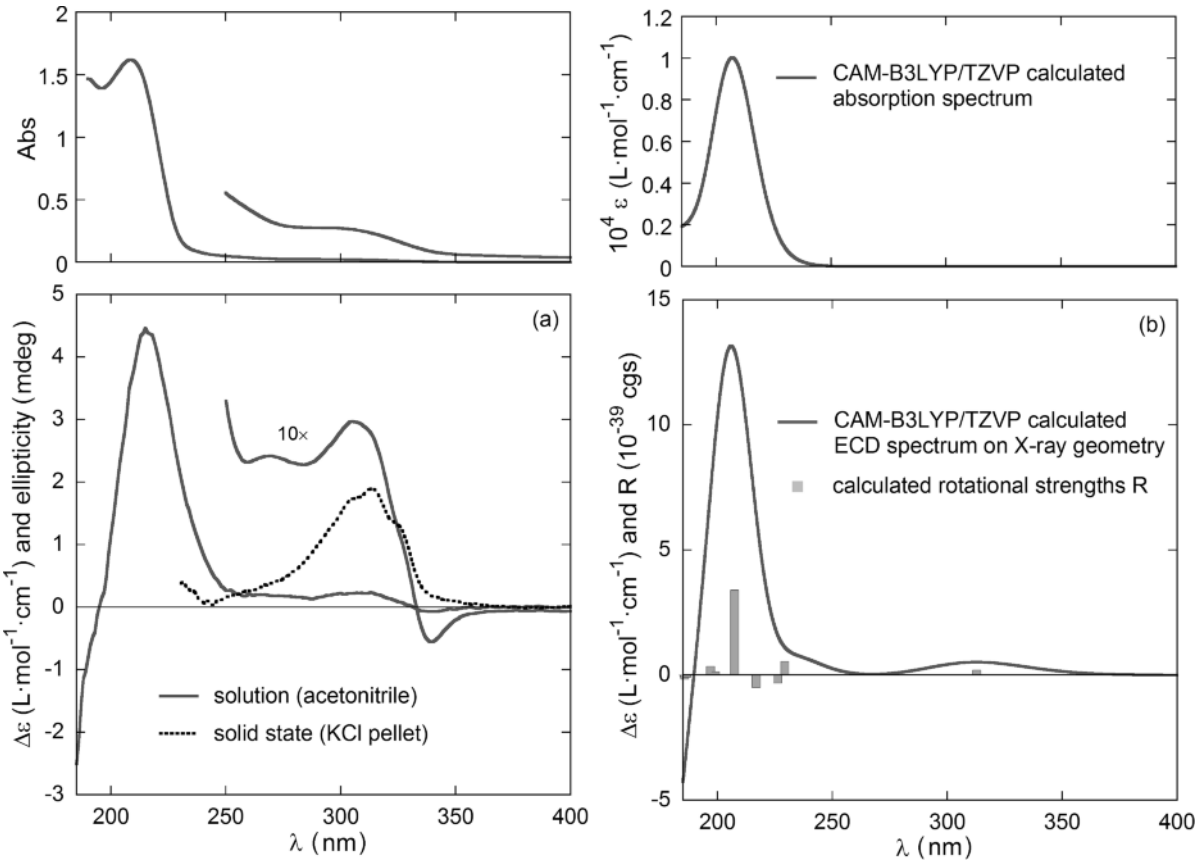

Fig. 3. Experimental (a, left) and calculated (b, right) absorption (top) and ECD spectra (bottom) of (+)-(1*S*,2*R*,4*R*,5*R*,6*S*,8*S*,9*R*,10*S*,13*S*,14*R*,17*S*,30*S*)-1-*O*-deacetyl-2-α-methoxykhayanolide E (**1**). Solution spectra measured on a 3.0 mM sample using 0.05 cm and 1 cm (expansions) cells. Calculated spectra obtained by CAM-B3LYP/TZVP calculations on the X-ray input geometries after application of a band-shape with 0.4 eV exponential half width, red-shifted by 10 nm.

Table 2. ^{1}H and ^{13}C NMR data, HMBC, and COSY correlations of **2** (CD_3OD).

Position	δ_H (mult., J in Hz)	δ_C	HMBC (H→C)	COSY (H→H)
1	–	85.2	–	–
2	4.47 (dd, 9.5, 6.5)	73.9	1,3,4,8,30	H-2/H-3,30
3	3.37 (d, 6.5)	80.1	2,4,5,29,30	H-3/H-2
4	–	43.5	–	–
5	3.18 (d, 8.5)	41.9	1,4,6,7,9,10,19,28,29	H-5/H-6
6	4.17 (d, 8.5)	72.3	4,5,7,10	H-6/H-5
7	–	176.9	–	–
8	–	88.3	–	–
9	2.11 (d, 9.0)	56.9	1,5,8,11,12,14,19,30	H-9/H-11
10	–	60.6	–	–
11	2.13 (d 9.0) 1.80 (m)	17.4	8,9,10,12,13	H-11/H-12
12	1.88 (d, 12.0) 0.87 (d, 12.0)	27.6	9,11,13,14,18	H-12/H-11
13	–	38.9	–	–
14	–	79.3	–	–
15	3.08 (d, 19.0) 2.78 (d, 19.0)	33.2	8,13,14,16	H-15a/H-15b
16	–	173.5	–	–
17	5.76 (s)	82. 6	12,13,14,18,20,21,22	–
18	1.09 (s)	15.3	12,13,14,17	–
19	1.21 (s)	18.3	1,5,9,10	–
20	–	122.2	–	–
21	7.50 (s)	142.4	17,20,22,23	–
22	6.45 (s)	111.1	17,20,21,23	–
23	7.46 (s)	144.4	20,21,22	–
28	1.00 (s)	15.2	3,4,5,29	–
29	1.86 (d, 12.0) 1.34 (d, 12.0)	46.1	1,3,4,5,10,30	H29a/H-29b
30	2.60 (d, 9.5)	64.6	1,2,3,8,9,14,29	H-30/H-2
7-OMe	3.73 (s)	52.6	7	–

that established for related khayanolides such as khayanolide A [19] and 1-*O*-acetylkhayanolide B (**5**) [20].

The IR spectrum of compound **2** was similar to that of **1**. The molecular formula $C_{27}H_{36}O_{10}$ was established by HREIMS which showed a molecular ion peak $[M]^+$ at $m/z = 518.2315$. The ^{1}H NMR spectrum of **2** (Table 2) was also similar to that of **1** except for the missing methoxy signal at $\delta = 3.48$. Additionally, it displayed two oxygenated methines at $\delta = 4.47$ (1H, dd, $J = 9.5$, 6.5 Hz) and 3.37 (1H, d, $J = 6.5$ Hz) which were correlated in the COSY spectrum as being vicinal to each other. The ^{13}C NMR spectrum of **2** (Table 2) showed a total of 27 carbon signals with the two oxymethines at $\delta = 80.1$ and 73.9. The above spectroscopic data showed close resemblance with that reported for khayanolide B [15]. The upfield shift of C-14 ($\delta = 79.3$) and the downfield shift of C-8 ($\delta = 88.3$) gave a clue about the cleavage of a bond between C-2 and C-14 with the formation of a new four-membered ring between C-2 and C-8 which was confirmed by HMBC correlations in which the CH_3-18 ($\delta = 1.09$) showed a correlation with C-14 ($\delta = 79.3$). Based on these evidences the compound was assigned the structure of **2** and named kigelianolide. The absolute configuration of (–)-**2** is assumed to be that shown in Fig. 1, corresponding to its analogs **1** and **3**, based on the isolation from the same source and on biogenetic considerations.

Limonoides are *nor*-triterpenes mostly found in the Meliaceae, Rutaceae, Cneoraceae and Simaroubaceae plant families. This class of compounds exhibits a range of biological activities including insecticidal, insect antifeedant, antibacterial, antifungal, antimalarial, anticancer, and antiviral activities on humans [21]. Several *Citrus* limonoids may provide substantial anticancer actions [22]. This class of compounds is receiving much attention towards their unusual structure and diverse biological activities.

Compounds **1**–**5** were evaluated for their enzyme inhibitory potential against enzymes AChE, BChE and LOX using eserine and baicalein (Aldrich, Seelze,

Table 3. AChE, BChE, and LOX inhibitory activities of compounds **1–5**[a].

Compound[b]	AChE (%)	AChE (IC_{50}) μM	BChE (%)	BChE (IC_{50}) μM	LOX (%)	LOX (IC_{50}) μM
1	46.6 ± 0.31	< 400	60.2 ± 0.91	228.5 ± 0.27	63.0 ± 0.16	281.2 ± 0.11
2	55.2 ± 0.33	< 400	66.7 ± 0.18	185.4 ± 0.38	54.3 ± 0.46	< 400
3	78.6 ± 0.74	137.5 ± 0.05	55.8 ± 0.55	< 400	45.2 ± 0.82	< 400
4	46.9 ± 0.55	< 400	59.9 ± 0.77	241.5 ± 0.11	62.5 ± 0.44	289.6 ± 0.14
5	61.8 ± 0.63	225.2 ± 0.22	65.3 ± 0.62	198.7 ± 0.15	52.2 ± 0.63	< 400
Eserine	91.3 ± 1.17	0.04 ± 0.0001	82.8 ± 1.09	0.85 ± 0.001	–	–
Baicalein	–	–	–	–	93.8 ± 1.2	22.4 ± 1.3

[a] All the measurements were done in triplicate, and statistical analysis was performed by Microsoft EXCEL 2003. Results are presented as mean $\pm$ *sem*; [b] all compounds were prepared in methanol with a concentration of 0.5 mM.

Germany) as positive controls. The results (Table 3) showed that the compounds were inhibitors of the used enzymes.

Experimental Section

General experimental procedures

Optical rotations were measured on a Jasco DIP-360 polarimeter. UV spectra were obtained in methanol on a U-3200 Schimadzu UV-240 spectrophotometer. Infrared (IR) spectra were recorded on a Shimadzu 460 spectrometer. ^{1}H (400, 500 MHz), ^{13}C NMR (100, 125 MHz) and 2D NMR (HMQC, HMBC and COSY; 400, 500 MHz) spectra were recorded on a Bruker spectrometer. The chemical shift values (δ) are reported in ppm, and the coupling constants (J) are in Hz. EIMS and HREIMS were recorded on a Finnigan (Varian MAT) JMS H $\times$ 110 instrument with a data system and a JMSA 500 mass spectrometer, respectively. Chromatographic separations were carried out using aluminum sheets pre-coated with silica gel 60 F_{254}(20×20 cm, 0.2 mm thick; E. Merck) for thin layer chromatography (TLC) and silica gel (230 – 400 mesh) for column chromatography. TLC plates were visualized under UV at 254 and 366 nm and by spraying with ceric sulfate solution and heating.

ECD spectra were recorded with a Jasco J-715 spectropolarimeter under the following conditions: scanning speed, 100 nm min^{-1}; time constant, 1 s; band width, 2 nm; 8 accumulations. Solid-state ECD spectra were obtained using the KCl pellet technique [16] using *ca.* 100 μg of compound and *ca.* 200 mg of oven-dried KCl. Rotation-dependent artifacts were checked by recording the spectrum upon four rotations of 90° of the disc around the light direction and vertical flip, which resulted in nearly identical ECD curves.

Plant material

Kigelia africana Benth was collected from Lal Sohanra (District Bahawalpur) in September 2010 and was identified by Dr. Muhammad Arshad (late), Plant Taxonomist, Cholistan Institute for Desert Studies (CIDS), The Islamia University of Bahawalpur, Pakistan, where a voucher specimen is deposited (KA/CIDS-404/10).

Extraction and isolation

The shade-dried powdered plant material of *Kigelia africana* was extracted thrice in methanol at room temperature. The crude methanolic extract was further divided into *n*-hexane-, and ethyl acetate/water-soluble fractions. The ethyl acetate-soluble fraction was subjected to column chromatography over silica gel using *n*-hexane/EtOAc, EtOAc, EtOAc/MeOH, and MeOH as eluents resulting in six fractions E_1–E_6. Fraction E_2 on gradient elution using 40% EtOAc in *n*-hexane to obtain deacetylkhayanolide E (**3**) and 45% EtOAc in *n*-hexane to purify 1-*O*-deacetyl-2α-methoxykhayanolide (**1**). Fraction E_3 on gradient elusion using 50% EtOAc in *n*-hexane provided 1-*O*-deacetyl-2α-hydroxykhayanolide E (**4**), 55% EtOAc in *n*-hexane provided 1-*O*-deacetyl-2α-methoxykhayanolide (**1**) and khayanolide B (**5**), respectively.

*1-O-Deacetyl-2-α-methoxykhayanolide E (**1**)*

Colorless crystalline solid (48 mg); $[\alpha]_D^{25} = +19.7$ ($c = 0.015$, MeOH). – UV (CH_3OH): λ_{max} (nm) = 210 (3.09). – IR (KBr): ν_{max} (cm^{-1}) = 3435, 2954, 1736, 1718, 1615, 1459, 1388, 1249, 1026, 983. –^{1}H and ^{13}C NMR, see Table 1. – HRMS ((+)-EI): m/z = 546.2110 (calcd. 546.2101 for $C_{28}H_{34}O_{11}$, $[M]^+$).

*Kigelianolide (**2**)*

Colorless amorphous powder (40 mg); $[\alpha]_D^{25} = -22.6$ ($c = 0.013$, MeOH). – UV (CH_3OH): λ_{max} (nm) = 211 (3.6). – IR (KBr): ν_{max} (cm^{-1}) = 3434, 2955, 1735, 1717, 1616, 1459, 1386, 1250, 1025, 985. –^{1}H and ^{13}C NMR data, see Table 2. – HRMS ((+)-EI): m/z = 518.2315 (calcd. 518.2308 for $C_{27}H_{36}O_{10}$, $[M]^+$).

Table 4. Selected geometric parameters in the molecular structure of **1**·1H$_2$O (Å, deg).

C1–O1	1.459(4)	C23–O10	1.209(3)
C2–O2	1.201(3)	C23–O9	1.338(3)
C3–O3	1.423(3)	C24–O9	1.470(3)
C4–C5	1.589(3)	C26–C27	1.333(4)
C6–C7	1.500(4)	C28–O11	1.357(4)
C7–O4	1.431(3)	C12–O8	1.413(3)
C11–O5	1.212(3)	C12–O6	1.416(3)
O1–C2–C3	111.9(2)	C16–C17–C18	114.9(2)
C2–C3–C4	110.6(2)	C17–C18–C19	111.8(2)
C7–C6–C5	102.9(2)	C24–C19–C20	105.89(18)
C6–C7–C8	104.7(2)	C2–O1–C1	116.4(3)
O8–C12–O6	105.63(18)	C12–O6–C14	115.8(2)
C23–O9–C24	122.99(18)	C12–O8–C20	109.50(17)

Crystal structure determination of ***1***·*1H$_2$O*

A colorless needle-shaped single crystal of **1** was grown in acetone by slow evaporation over a period of three days. It was found to cyrstallize with one interstitial water molecule. The relative structure of the molecule was confirmed by single-crystal X-ray diffraction (Fig. 2). Due to the absence of strong anomalous scatterers in the molecule, the Flack x parameter was not reliable enough to ascertain the absolute configuration. Hence electronic circular dichroism (ECD) spectroscopy was exploited to determine the absolute configuration. Table 4 lists selected geometric parameters of the molecule in the solid state. *Crystal structure data:* $C_{28}H_{36}O_{12}$,$M_r = 564.57$, needle-shaped colorless crystal, $0.30 \times 0.25 \times 0.18$ mm^3, orthorhombic space group $P2_12_12_1$, $a = 7.7524(3)$, $b = 17.5899(7)$, $c = 19.3138(9)$ Å, $V = 2633.71(19)$ Å^3, $Z = 4$, $\rho_{calcd.} = 1.42$ g cm^{-3}, μ(MoK_α) = 0.1 mm^{-1}, multi-scans absorption correction, $T_{min} = 0.967$, $T_{max} = 0.980$, MoK_α radiation, $\lambda = 0.71073$ Å, $T = 296(2)$ K, ω scans, 21514 measured reflections, ($\pm h, \pm k, \pm l$), $\theta_{max} = 25.5°$, $\theta_{min} = 1.6°$, 4914 independent ($R_{int} = 0.044$) and 3882 observed reflections, [$I \geq 2\ \sigma(I)$], 375 refined parameters, $S = 1.01$, $R = 0.043$, $wR2 = 0.101$, Flack x parameter $= -1.0(10)$, max./min. residual electron density $0.24/-0.28$ e Å^{-3}. Hydrogen atoms were calculated and refined as riding atoms. The data set was collected with a Bruker Kappa CCD detector diffractometer. Programs used: Data collection: APEX2 [23]; cell refinement: SAINT [23]; data reduction: SAINT [23]; absorption correction: SADABS [24], structure solution and refinement: SHELXS/L-97 [25]; graphics: ORTEP3 for windows [26].

CCDC 933705 contains the supplementary crystallographic data for this paper. This data can be obtained free of charge from The Cambridge Crystallographic Data Center *via* www.ccdc.cam.ac.uk/data_request/cif.

Computational studies

DFT and TDDFT calculations were run with GAUSSIAN'09 [27] with default grids and convergence criteria. The X-ray structure of compound **1** was partially optimized by DFT at the B3LYP/6-31G(d) level [28] by restraining the positions of all heavy atoms and optimizing only hydrogen atoms. This partial optimization is necessary because of the artificially short C–H and O–H bonds found in X-ray structure determinations. TDDFT calculations were run using several functionals (B3LYP, CAM-B3LYP, BH&HLYP) and basis sets (SVP, TZVP) [28], leading to consistent results in all cases; only CAM-B3LYP/TZVP data are discussed in the text. ECD spectra were generated by applying a Gaussian band shape with 0.5 eV exponential half-width, using the program SPECDIS [29]. Dipole-length rotational strengths were employed to construct ECD spectra; the difference with dipole-velocity values was checked to be minimal for all relevant transitions.

Acetylcholinesterase assay

The acetylcholinesterase (AChE) inhibition activity was determined according to the method used by Ellman [30] with slight modifications. The percent inhibition was calculated by the help of following equation;

$$\text{Inhibition (\%)} = \frac{\text{Control} - \text{Test}}{\text{Control}} \times 100$$

Butyrylcholinesterase assay

The butyrylcholinesterase (BChE) inhibition activity was determined according to the method used by Ellman [30] with slight modifications. The percent inhibition was calculated with the help of following equation;

$$\text{Inhibition (\%)} = \frac{\text{Control} - \text{Test}}{\text{Control}} \times 100$$

IC_{50} values (concentration at which there is 50% enzyme inhibition) of compounds were calculated using the EZ-FIT Enzyme Kinetics software (Perella Scientific Inc., Amherst, MA, USA).

Lipoxygenase assay

Lipoxygenase (LOX) activity was assayed according to the reported method [31], but with slight modifications. All reactions were performed in triplicates. Baicalein (0.5 mM well^{-1}) was used as a positive control. The percentage inhibition was calculated by the formula given below;

$$\text{Inhibition (\%)} = \frac{\text{Control} - \text{Test}}{\text{Control}} \times 100$$

[1] G. Cordell, *Phytochemistry* **2000**, *56*, 463 – 480.
[2] A. Oliver-Bever, *Medicinal Plants in Tropical West Africa*, Cambridge University Press, Cambridge, **1986**, pp. 240 – 245.
[3] S. J. Jackson, P. J. Houghton, S. Retsas, A. Photiou, *Planta Med.* **2000**, *66*, 758 – 761.
[4] S. V. K. Moideen, P. J. Houghton, P. Rock, S. L. Croft, F. Aboagye-Nyame, *Planta Med.* **1999**, *65*, 536 – 540.
[5] D. N. Akunyili, P. J. Houghton, A. J. Roman, *Ethnopharmacol.* **1991**, *35*, 173 – 177.
[6] P. J. Houghton, A. Photiou, S. Uddin, P. Shah, M. Browning, S. J. Jackson, S. Retsas, *Planta Med.* **1994**, *60*, 430 – 433.
[7] H. Weenen, M. H. H. Nkunya, D. H. Bray, L. B. Mwasumbi, L. S. Kinabo, V. A. E. B. Kilimali, *Planta Med.* **1990**, *56*, 368 – 370.
[8] O. J. Owolabi, E. K. Omogbai, *Afr. J. Biotechnol.* **2007**, *6*, 582 – 585.
[9] M. T. Olaive, J. B. Rocha, *Exp. Toxical. Pathol.* **2007**, *58*, 433 – 438.
[10] J. D. Msouthi, D. Mangombo, *Hamdard* **1983**, *26*, 94 – 100.
[11] O. J. Owolabi, F. C. Amaechina, A. B. Eledan, *Afr. J. Med. Plant Res.* **2008**, *2*, 20 – 23.
[12] D. Akunyili, P. Houghton, *Phytochemistry* **1993**, *32*, 1015 – 1018.
[13] H. Zhang, O. A. Odeku, X. Wang, J. Yue, *Phytochemistry* **2008**, *69*, 271 – 275.
[14] B. Zhang, S. Yang, S. Yin, C. Zhang, Y. Wu, J. Yue, *Phytochemistry* **2009**, *70*, 1305 – 1308.
[15] S. A. M. Abdelgaleil, H. Okamura, T. Iwagawa, A. Sato, I. Miyahara, M. Doe, M. Nakatani, *Tetrahedron* **2001**, *57*, 119 – 126.
[16] G. Pescitelli, T. Kurtán, U. Flörke, K. Krohn, *Chirality* **2009**, *21*, E181–E201.
[17] J. Autschbach, L. Nitsch-Velasquez, M. Rudolph, *Top. Curr. Chem.* **2011**, *298*, 1 – 98.
[18] G. Pescitelli, L. D. Bari, N. Berova, *Chem. Soc. Rev.* **2011**, *40*, 4603 – 4625.
[19] M. Nakatani, S. A. M. Abdelgaleil, H. Okamura, T. Iwagawa, A. Sato, M. Doe, *Tetrahedron Lett.* **2000**, *41*, 6473 – 6477.
[20] H. Zhang, J. Tan, D. VanDerveer, X. Wang, M. J. Wargovich, F. Chen, *Phytochemistry* **2009**, *70*, 294 – 299.
[21] R. Amit, S. Shailendra, *Biol. Pharm. Bull.* **2006**, *29*, 191 – 201.
[22] E. Sohail, E. Ahmed, M. Kiku, W. Chae, *J. Sci. Food Agric.* **2006**, *86*, 339 – 345.
[23] Bruker Analytical X-ray Instruments Inc., Madison, Wisconsin (USA) **2009**.
[24] G. M. Sheldrick, SADABS, Program for Empirical Absorption Correction of Area Detector Data, University of Göttingen, Göttingen (Germany) **2002**.
[25] G. M. Sheldrick, *Acta Crystallogr.* **2008**, *A64*, 112 – 122.
[26] C. K. Johnson, M. N. Burnett, ORTEP3, Oak Ridge Thermal Ellipsoid Plot Program for Crystal Structure Illustrations, Rep. ORNL-6895, Oak Ridge National Laboratory, Oak Ridge, TN (USA) **1996**. Windows version: L. J. Farrugia, University of Glasgow, Glasgow, Scotland (U. K.) **1999**.
[27] M. J. Frisch, G. W. Trucks, H. B. Schlegel, G. E. Scuseria, M. A. Robb, J. R. Cheeseman, G. Scalmani, V. Barone, B. Mennucci, G. A. Petersson, H. Nakatsuji, M. Caricato, X. Li, H. P. Hratchian, A. F. Izmaylov, J. Bloino, G. Zheng, J. L. Sonnenberg, M. Hada, M. Ehara, K. Toyota, R. Fukuda, J. Hasegawa, M. Ishida, T. Nakajima, Y. Honda, O. Kitao, H. Nakai, T. Vreven, J. A. Montgomery, Jr., J. E. Peralta, F. Ogliaro, M. Bearpark, J. J. Heyd, E. Brothers, K. N. Kudin, V. N. Staroverov, R. Kobayashi, J. Normand, K. Raghavachari, A. Rendell, J. C. Burant, S. S. Iyengar, J. Tomasi, M. Cossi, N. Rega, J. M. Millam, M. Klene, J. E. Knox, J. B. Cross, V. Bakken, C. Adamo, J. Jaramillo, R. Gomperts, R. E. Stratmann, O. Yazyev, A. J. Austin, R. Cammi, C. Pomelli, J. W. Ochterski, R. L. Martin, K. Morokuma, V. G. Zakrzewski, G. A. Voth, P. Salvador, J. J. Dannenberg, S. Dapprich, A. D. Daniels, Ö. Farkas, J. B. Foresman, J. V. Ortiz, J. Cioslowski, D. J. Fox, GAUSSIAN09 (revision A.02), Gaussian, Inc., Wallingford CT (USA), **2009**.
[28] All references about DFT functionals and basis sets can be found in the on-line documentation for GAUSSIAN09 at www.gaussian.com/g_tech/g_ur/g09help.htm.
[29] T. Bruhn, Y. Hemberger, A. Schaumlöffel, G. Bringmann, SPECDIS (version 1.53), University of Würzburg, Würzburg (Germany), **2012**.
[30] G. L. Ellman, K. D. Courtney, V. Andres, R. M. Featherstone, *Biochemical. Pharmacol.* **1961**, *7*, 88 – 90.
[31] A. L. Tappel, *Arch. Biochem. Biophy.* **1953**, *44*, 378 – 395.